10.1071/ES24027
Journal of Southern Hemisphere Earth Systems Science

Supplementary Material

Biogenic CO_2 flux uncertainty: numerical experiments and validation over south-eastern South America

Nahuel E. Bautista[A,B,*], *Juan J. Ruiz*[B,C,D], *Paola V. Salio*[B,C,D], *Lucas J. Burgos*[E] and *María I. Gassmann*[A,B]

[A]Consejo Nacional de Investigaciones Científicas y Técnicas (CONICET), Buenos Aires, Argentina

[B]Departamento de Ciencias de la Atmósfera y los Océanos (DCAO), Facultad de Ciencias Exactas y Naturales, Universidad de Buenos Aires, Avenida Intendente Güiraldes 2160, C1428EGA, Ciudad Autónoma de Buenos Aires, Argentina

[C]Centro de Investigaciones del Mar y la Atmósfera (CIMA), CONICET–Universidad de Buenos Aires, Buenos Aires, Argentina

[D]Instituto Franco–Argentino de Estudios sobre el Clima y sus Impactos (IFAECI), International Research Laboratory (IRL) 3351, Centre de la Recherche Scientifique (CNRS)–CONICET–Institut de Recherche pour le Développement (IRD)–Universidad de Buenos Aires (UBA), Buenos Aires, Argentina

[E]Departamento de Tecnología, Universidad Nacional de Luján (UNLu), Buenos Aires, Argentina

*Correspondence to: Email: nbautista@at.fcen.uba.ar

1. Station locations, altitudes and sounding launching times

Table S1: Weather stations used to validate T2 and PP estimated by the scenarios.

Source	Station name	Latitude	Longitude	Elevation (m ASL)
SMN	BAHIA BLANCA AERO	-38.73	-62.02	83
SMN	CATAMARCA AERO	-28.6	-65.77	454
SMN	CERES AERO	-29.88	-61.95	88
SMN	CONCORDIA AERO	-31.3	-58.02	38
SMN	CORDOBA AERO	-31.32	-64.22	474
SMN	DOLORES AERO	-36.35	-57.73	9
SMN	EZEIZA AERO	-34.82	-58.53	20
SMN	GENERAL PICO AERO	-35.7	-63.75	145
SMN	GUALEGUAYCHU AERO	-33	-58.62	21
SMN	JUNIN AERO	-34.55	-60.92	81
SMN	LABOULAYE AERO	-34.13	-63.37	137
SMN	MAR DEL PLATA AERO	-37.93	-57.58	21
SMN	MARCOS JUAREZ AERO	-32.7	-62.15	114
SMN	MONTE CASEROS AERO	-30.27	-57.65	54
SMN	PASO DE LOS LIBRES AERO	-29.68	-57.15	70
SMN	POSADAS AERO	-27.37	-55.97	125
SMN	RECONQUISTA AERO	-29.18	-59.7	53
SMN	RESISTENCIA AERO	-27.45	-59.05	52
SMN	RIO CUARTO AERO	-33.12	-64.23	421
SMN	ROSARIO AERO	-32.92	-60.78	25
SMN	SAN LUIS AERO	-33.27	-66.35	713
SMN	SANTA ROSA AERO	-36.57	-64.27	191
SMN	SANTIAGO DEL ESTERO AERO	-27.77	-64.3	199
SMN	SAUCE VIEJO AERO	-31.7	-60.82	18
SMN	TANDIL AERO	-37.23	-59.25	175
SMN	VILLA REYNOLDS AERO	-33.73	-65.38	486
INTA	25 de Mayo - EEA Pergamino	-35.48	-60.13	85
INTA	Arrecifes - EEA Pergamino	-34.05	-60.14	36
INTA	Bordenave - EEA Bordenave	-37.75	-63.08	202
INTA	Calchaqui - EEA Reconquista	-29.88	-60.24	70
INTA	Catuna - EEA La Rioja	-30.96	-66.17	497
INTA	Curuzu Cuatia - EEA Mercedes	-29.87	-58.11	80
INTA	Dean Funes - EEA Manfredi	-30.34	-64.32	701
INTA	Du Graty - EEA Sáenz Peña	-27.7	-60.91	89
INTA	Federal - EEA Concordia	-30.93	-58.77	65
INTA	La Cigüeña - EEA Reconquista	-29.25	-61.02	67
INTA	La Dulce - EEA Balcarce	-38.34	-59.01	72
INTA	Las Tunas - EEA Paraná	-31.87	-59.68	83
INTA	Lincoln - EEA Villegas	-34.84	-61.6	110
INTA	Los Juríes - EEA E Santiago	-28.61	-62.16	78
INTA	Mercedes - EEA Mercedes	-29.2	-58.04	99
INTA	Quimilí - EEA E Santiago	-27.54	-62.35	137
INTA	Rafaela - EEA Rafaela	-31.2	-61.5	90
INTA	Rio Colorado - EEA Alto Valle	-39.02	-64.08	79
INTA	Villa Dolores - EEA Manfredi	-31.94	-65.22	707

Table S2: Weather stations used to validate SWDOWN estimated by the scenarios.

Source	Station name	Latitude	Longitude	Elevation (m ASL)
INTA	Balcarce	-37.76	-58.3	133
INTA	Barrow	-38.32	-60.24	72
RELAMPAGO-CACTI	Berrotaran	-32.47	-64.4	635
SMN	BsAs	-34.58	-58.48	18
Mar Chiquita	Mar Chiquita	-37.7	-57.42	1
INTA	Concepción	-32.49	-58.35	22
RELAMPAGO-CACTI	Laborde	-33.16	-62.4	114
INTA	Luján	-34.59	-59.06	31
RELAMPAGO-CACTI	Marcos Juárez (Alfalfa)	-32.72	-62.07	112
RELAMPAGO-CACTI	Ordoñez	-32.8	-62.96	145
INTA	Paraná	-31.85	-60.54	102
INTA	Pergamino	-33.94	-60.55	57
RELAMPAGO-CACTI	San Francisco	-31.28	-62.36	111
RELAMPAGO-CACTI	Villa Chacay	-32.87	-64.89	1081

Table S3: Launching position of the radiosondes used to validate PBL temperatures estimated by the scenarios.

Source	Station name	Lati-tude	Longi-tude	Hour (sunny and cloudy; hours UTC)	Hour (rainy; hours UTC)
SMN / RELAMPAGO-CACTI	CORDOBA AERO	-31.32	-64.22	11:27:55; 23:28:52	05:31:17; 08:30:42; 11:30:26; 14:31:23; 17:30:13; 23:30:30
SMN / RELAMPAGO-CACTI	EZEIZA AERO	-34.82	-58.53	11:37:31	11:38:08
SMN / RELAMPAGO-CACTI	SANTA ROSA AERO	-36.57	-64.27	11:11:27	11:11:33
SMN / RELAMPAGO-CACTI	VILLA MARIA DEL RIO SECO	-29.9	-63.68	8:30:24	05:30:56; 08:27:02; 11:31:47; 14:31:19; 17:31:02

2. 2-m air temperatures (T2)

In this section we briefly analyse the spatial and temporal variations in T2 errors. Fig. S1–S3 show that ERA5 had the greatest bias in areas with complex topography along the western regions of the country. Moreover, it underestimated more than the WRF simulations their nocturnal cooling rate, which resulted in their WRF temperatures being closer to the observations (Fig. S4). As a consequence, the mean t-test of the errors between stations above and below 200 m resulted in lower P-values for ERA5 in each case. This is probably due to a more accurate representation of the topography by the former model. For example, at the station located at 28.50°S, 66.77°W, and 454 m ASL (Catamarca), WRF represents it at 465 m ASL whereas ERA5 does at 1318 m ASL. Therefore, WRF provided better estimates of T2 in areas with complex topography, but there were small differences with ERA5 in sites surrounded by flat terrain.

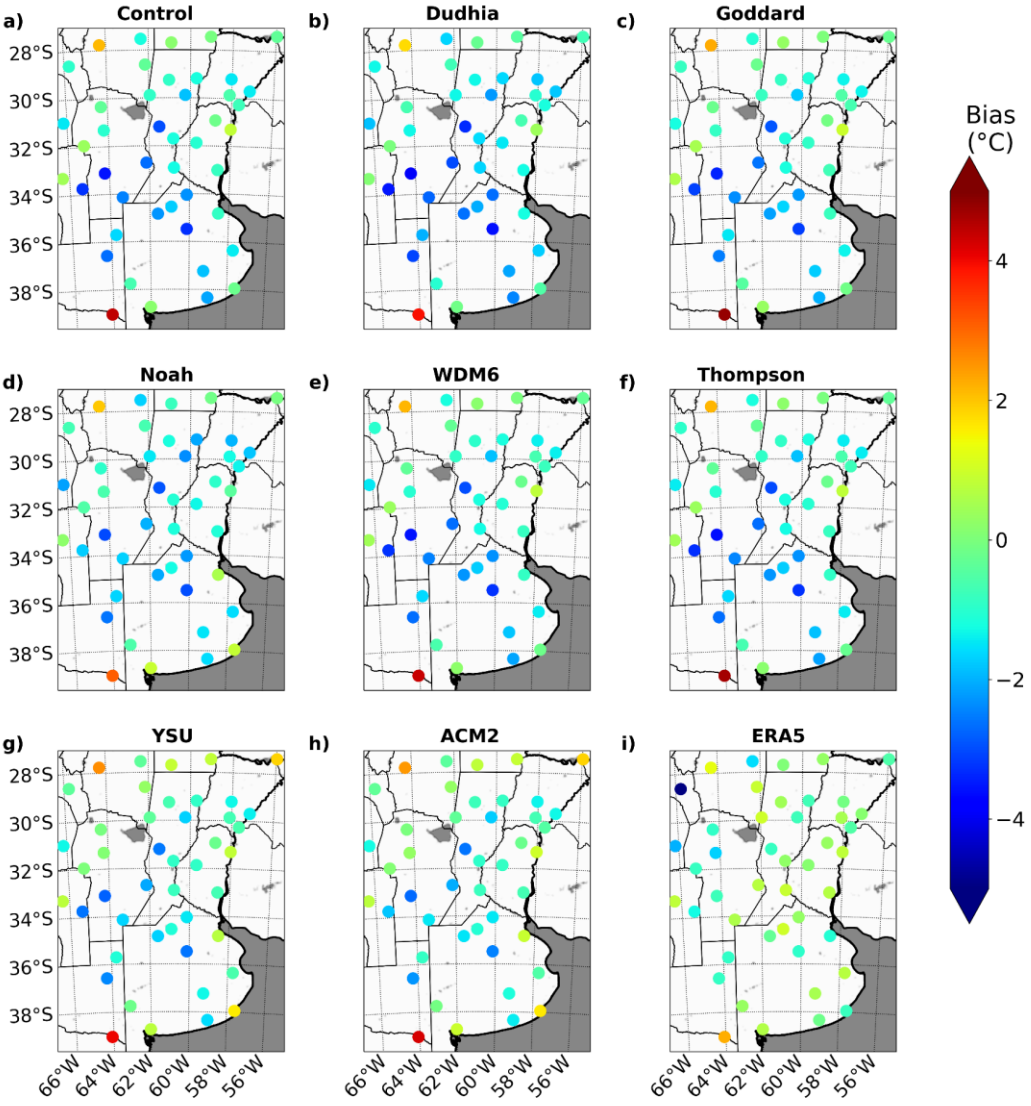

Fig. S1: T2 bias in the sunny case for each station.

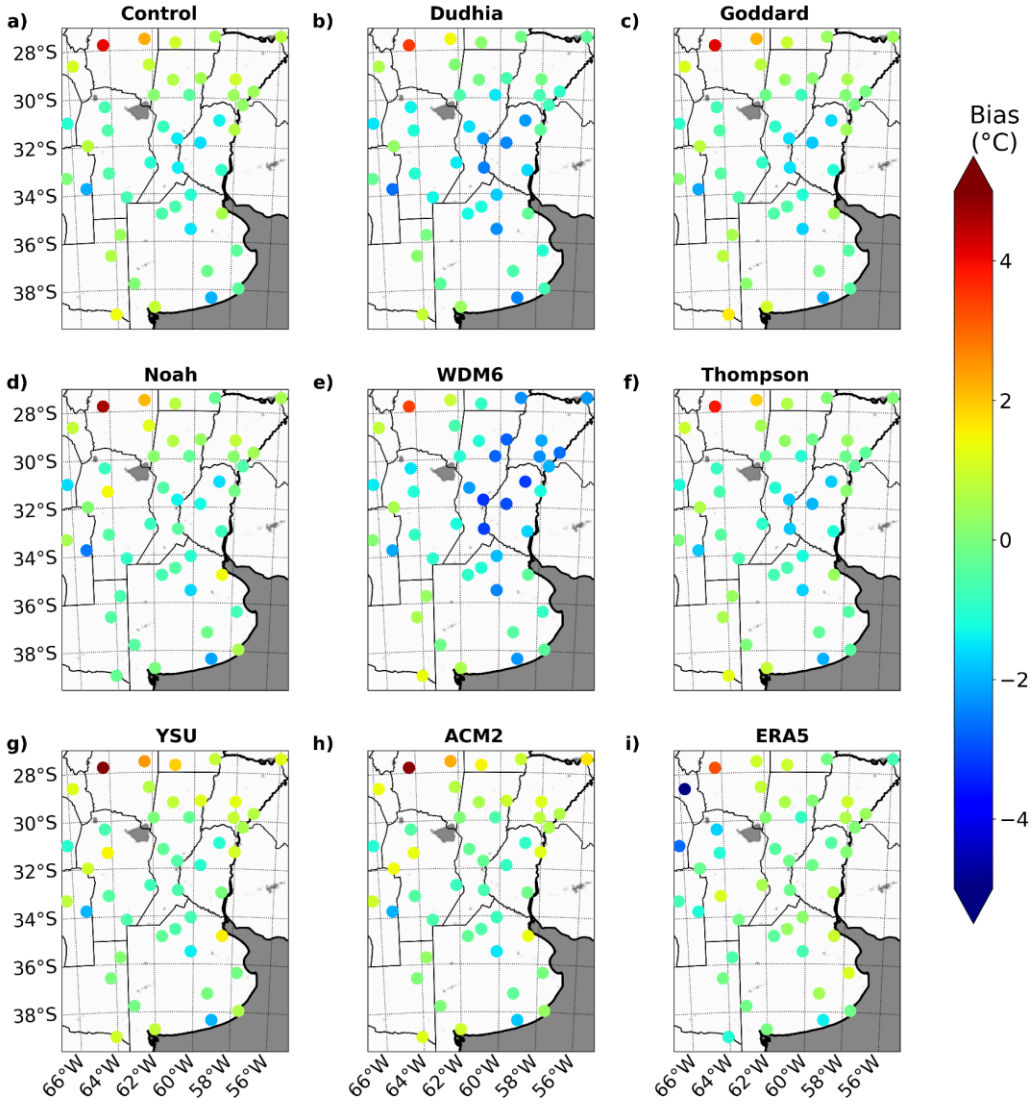

Fig. S2: T2 bias in the Cloudy case for each station.

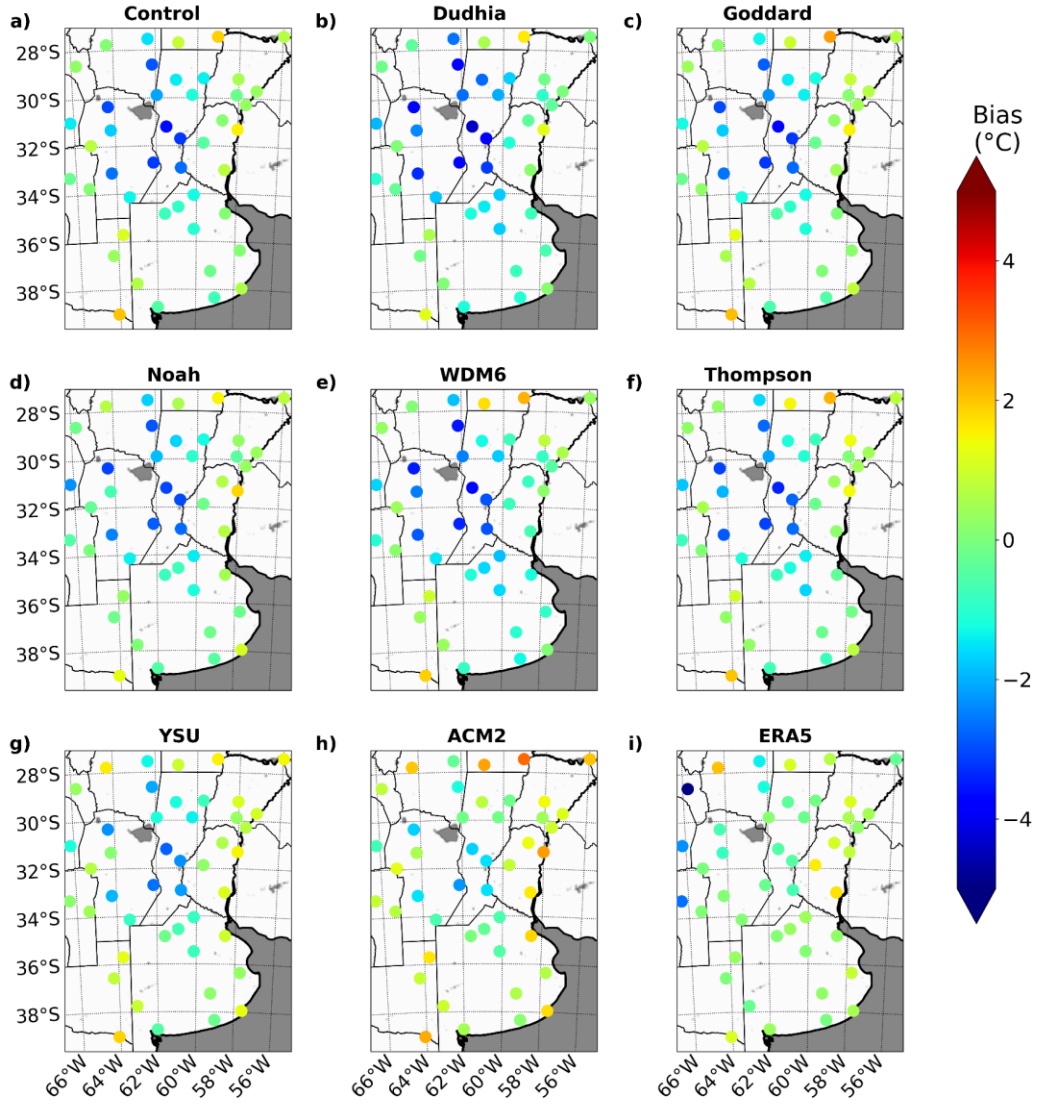

Fig. S3: T2 bias in the Rainy case for each station.

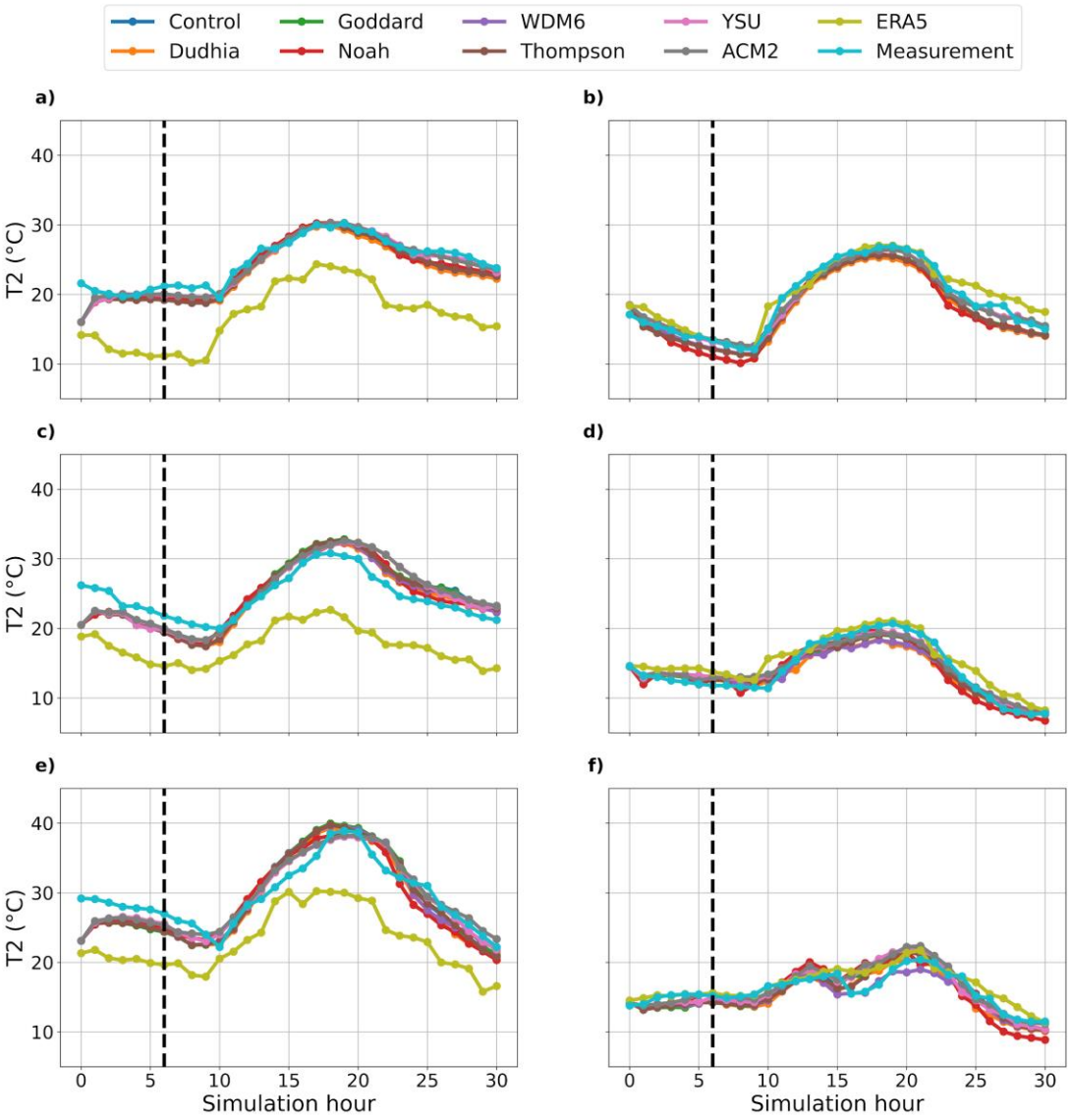

Fig. S4: T2 time series for a, c, e) Catamarca and b, d, f) Dolores stations in the a–b) Sunny, c–d) Cloudy and e–f) Rainy cases. The vertical dotted line is the model spin-up (6 h).

Table S4: Results of the means t-test performed between the RMSE of stations located below or above 200 m respectively.

Case	Model	*T*-statistic	*P*-value	Mean below 200 m	Mean above 200 m	s.d. below 200 m	s.d. above 200 m	Number below 200 m	Number above 200 m
Sunny	Control	-0.207	0.837	2.245	2.322	0.986	0.946	36	9
Sunny	Dudhia	-0.006	0.995	2.487	2.489	0.936	1.042	36	9
Sunny	Goddard	-0.169	0.866	2.191	2.255	1.017	0.894	36	9
Sunny	Noah	-0.168	0.867	2.125	2.172	0.726	0.732	36	9
Sunny	WDM6	-0.227	0.821	2.239	2.323	0.98	0.949	36	9
Sunny	Thompson	-0.191	0.85	2.253	2.326	1.004	0.949	36	9
Sunny	YSU	-0.046	0.963	2.173	2.189	0.906	0.833	36	9
Sunny	ACM2	0.039	0.969	2.219	2.205	0.939	0.79	36	9
Sunny	ERA5	-2.625	0.012	1.948	2.945	0.69	1.746	36	9
Cloudy	Control	-0.843	0.404	1.933	2.218	0.954	0.546	36	9
Cloudy	Dudhia	-0.664	0.51	2.093	2.32	0.964	0.537	36	9
Cloudy	Goddard	-0.643	0.523	1.946	2.172	0.991	0.56	36	9
Cloudy	Noah	-0.815	0.419	1.826	2.071	0.851	0.454	36	9
Cloudy	WDM6	0.962	0.341	2.562	2.219	1.018	0.484	36	9
Cloudy	Thompson	-0.749	0.458	1.928	2.182	0.959	0.52	36	9
Cloudy	YSU	-0.833	0.409	1.999	2.302	1.039	0.466	36	9
Cloudy	ACM2	-1.055	0.297	1.96	2.333	1.001	0.541	36	9
Cloudy	ERA5	-2.61	0.012	1.712	2.63	0.63	1.635	36	9
Rainy	Control	-0.894	0.376	2.158	2.441	0.856	0.713	36	9
Rainy	Dudhia	-1.069	0.291	2.325	2.755	1.052	1.06	36	9
Rainy	Goddard	-0.877	0.385	2.246	2.529	0.877	0.716	36	9
Rainy	Noah	-0.291	0.772	2.28	2.367	0.78	0.817	36	9
Rainy	WDM6	-1.563	0.125	2.223	2.772	0.906	0.984	36	9
Rainy	Thompson	-1.289	0.204	2.138	2.526	0.809	0.712	36	9
Rainy	YSU	0.172	0.864	2.134	2.091	0.701	0.407	36	9
Rainy	ACM2	0.499	0.62	2.069	1.94	0.752	0.197	36	9
Rainy	ERA5	-2.779	0.008	1.67	2.648	0.656	1.593	36	9

3. Shortwave incoming radiation at the surface (SWDOWN)

In this section we summarise the spatial and temporal variation of SWDOWN errors. Fig. S5 shows that the WRF simulations and ERA5 had a positive bias in the sunny case in the stations located at 32.80°S, 62.96°W (Ordoñez) and 38.32°S, 60.24°W (Berrotaran). However, Fig. S6–S7 show very different biases for each station across different configurations without any spatial pattern in them. Regarding the temporal variability of the errors, they were higher at the hours when the front was passing through each site. In consequence, the best configuration to estimate SWDOWN depended on each station location and on the accuracy of the configuration to simulate the position of the front.

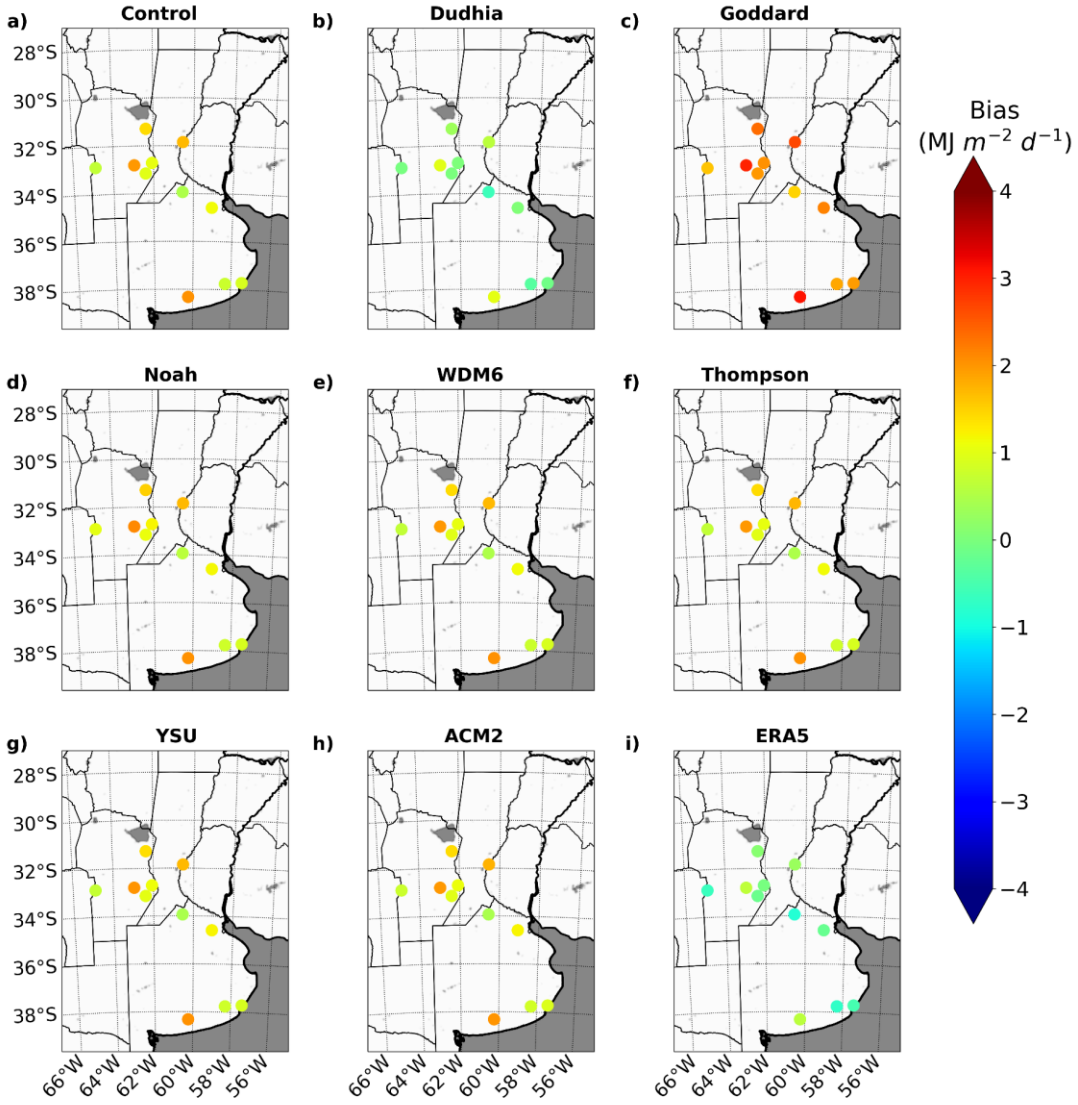

Fig. S5: SWDOWN 24-hour sum bias in the Sunny case for each station.

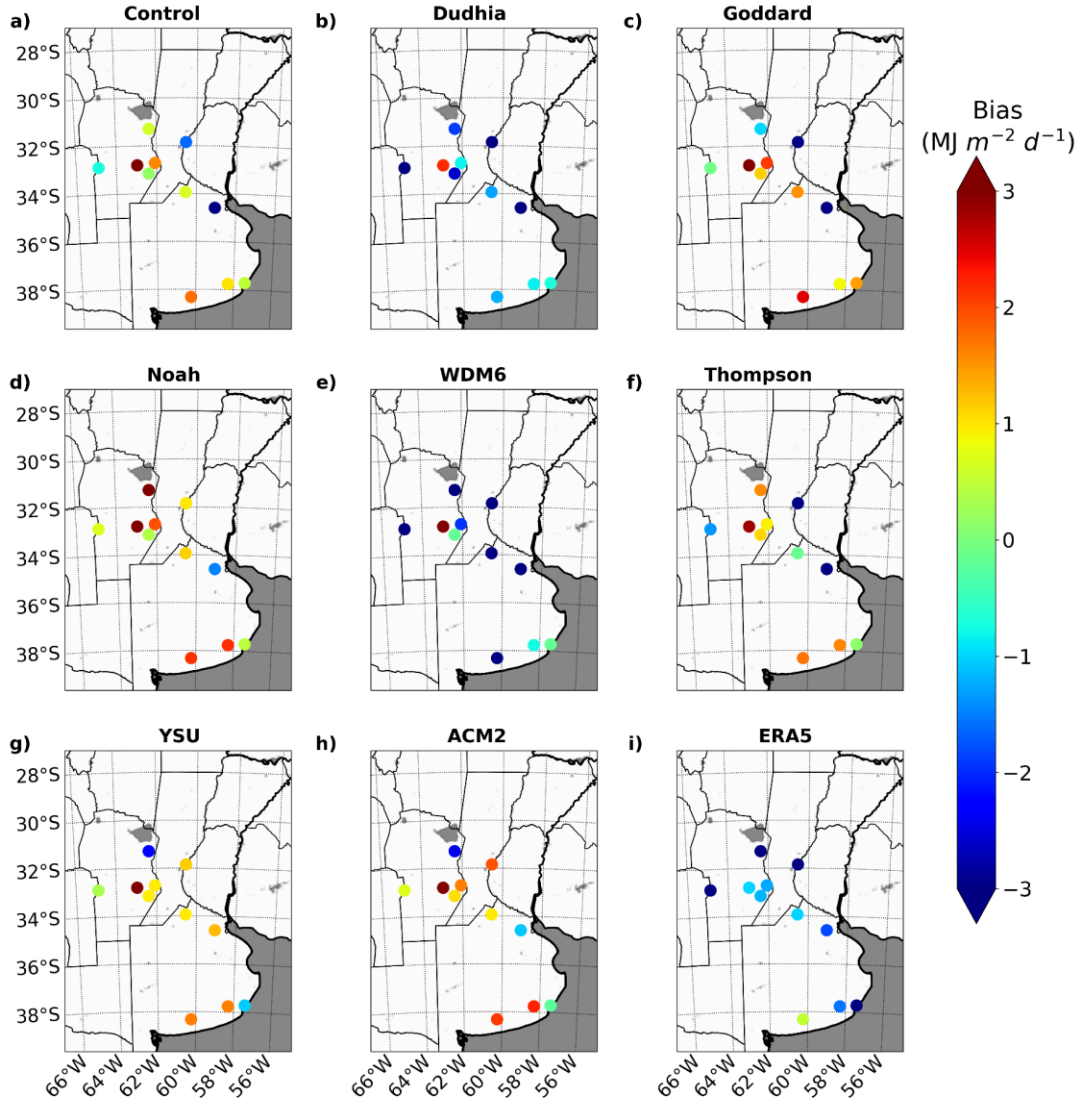

Fig. S6: SWDOWN 24-hour sum bias in the Cloudy case for each station.

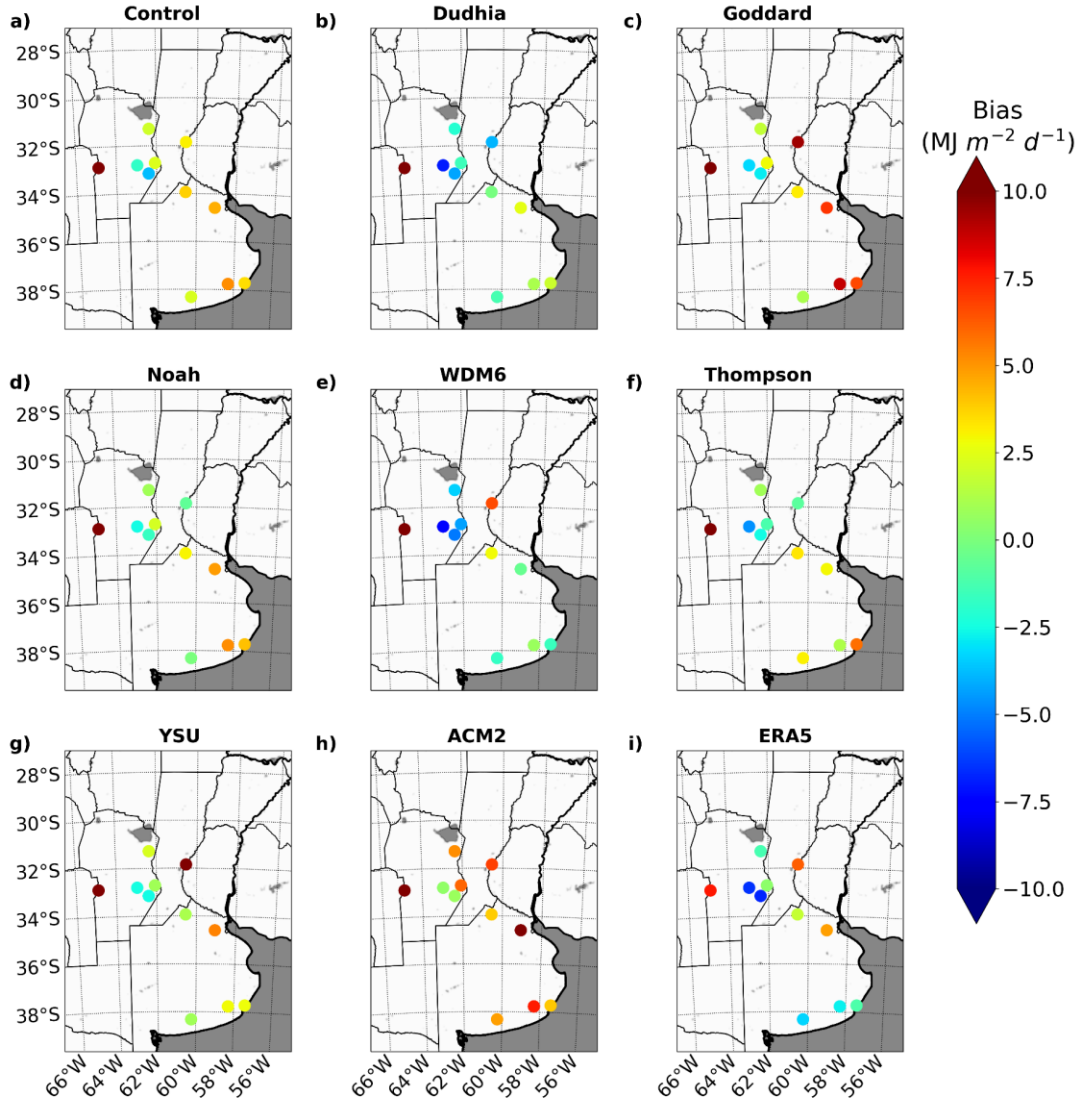

Fig. S7: SWDOWN 24-hour sum bias in the rainy case for each station.

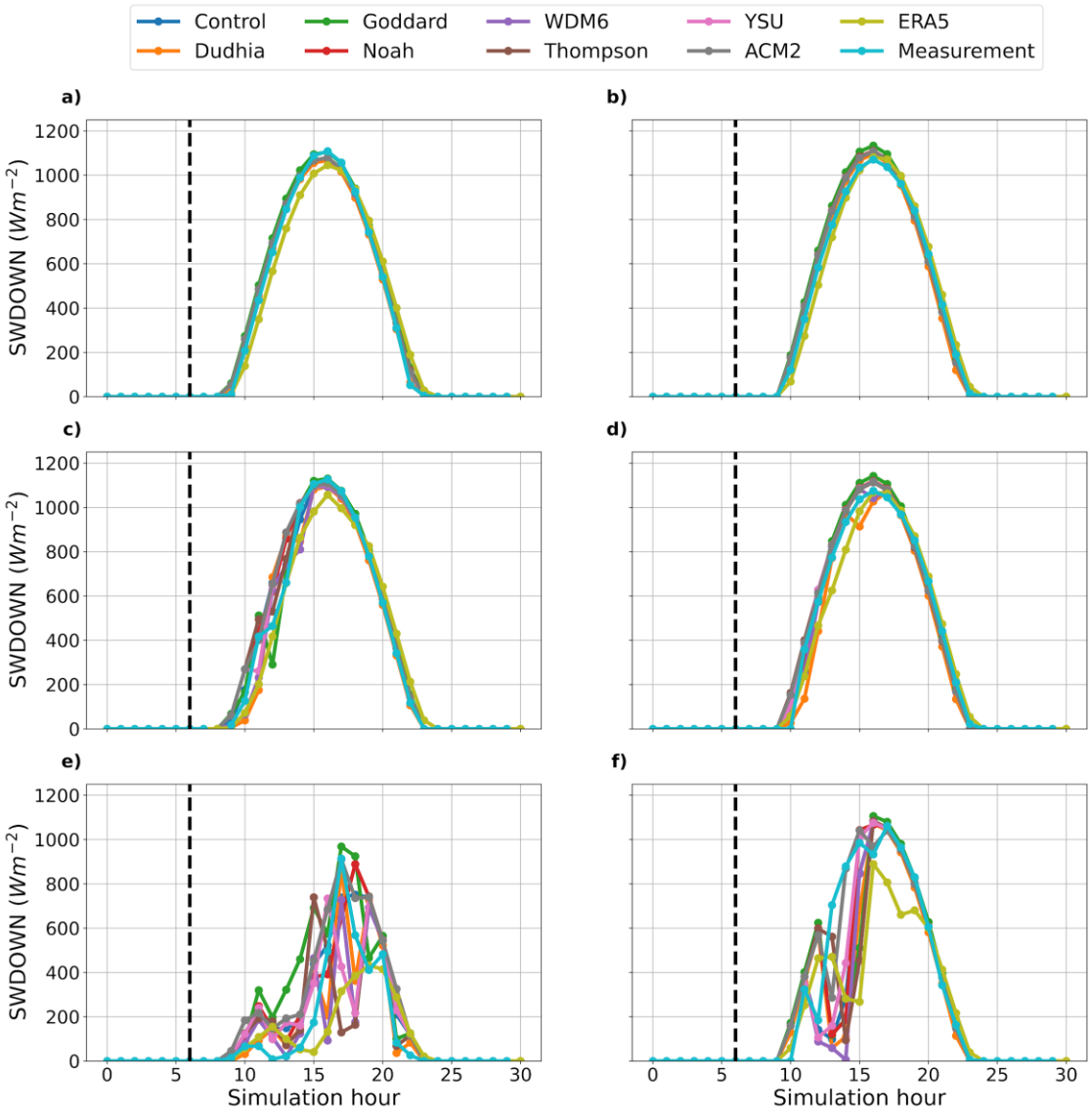

Fig. S8: SWDOWN time series for a, c, e) Balcarce and b, d, f) Luján stations in the a–b) sunny, c–d) cloudy and e–f) rainy cases. The vertical dotted line is the model spin-up (6 hours).

4. Precipitation (PP)

In this section we briefly analyze the spatial variation of PP errors. These variations were mainly associated with the area covered by the mesoscale convective system, with Control and Dudhia producing a larger and more intense convective system and with ACM2 and Thompson producing weaker and smaller ones (Figs. S9-10). The same pattern was also found in ERA5, which had a similar bias in the stations located far from the mesoscale system. Consequently, the most important factor that determined the best WRF configuration to estimate PP was its accuracy in simulating the PP from mesoscale system.

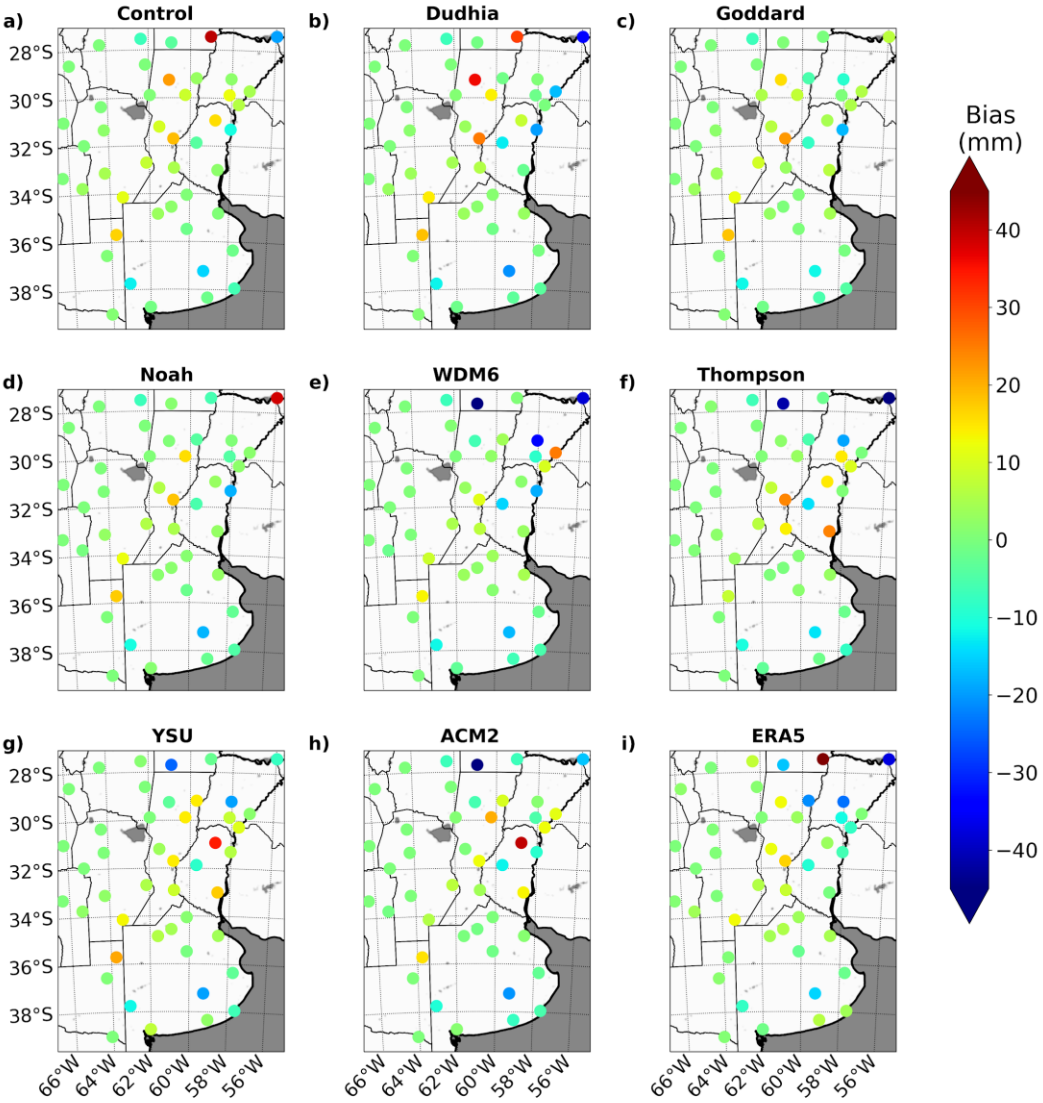

Fig. S9: 24-hour accumulated PP bias in the rainy case for each station.

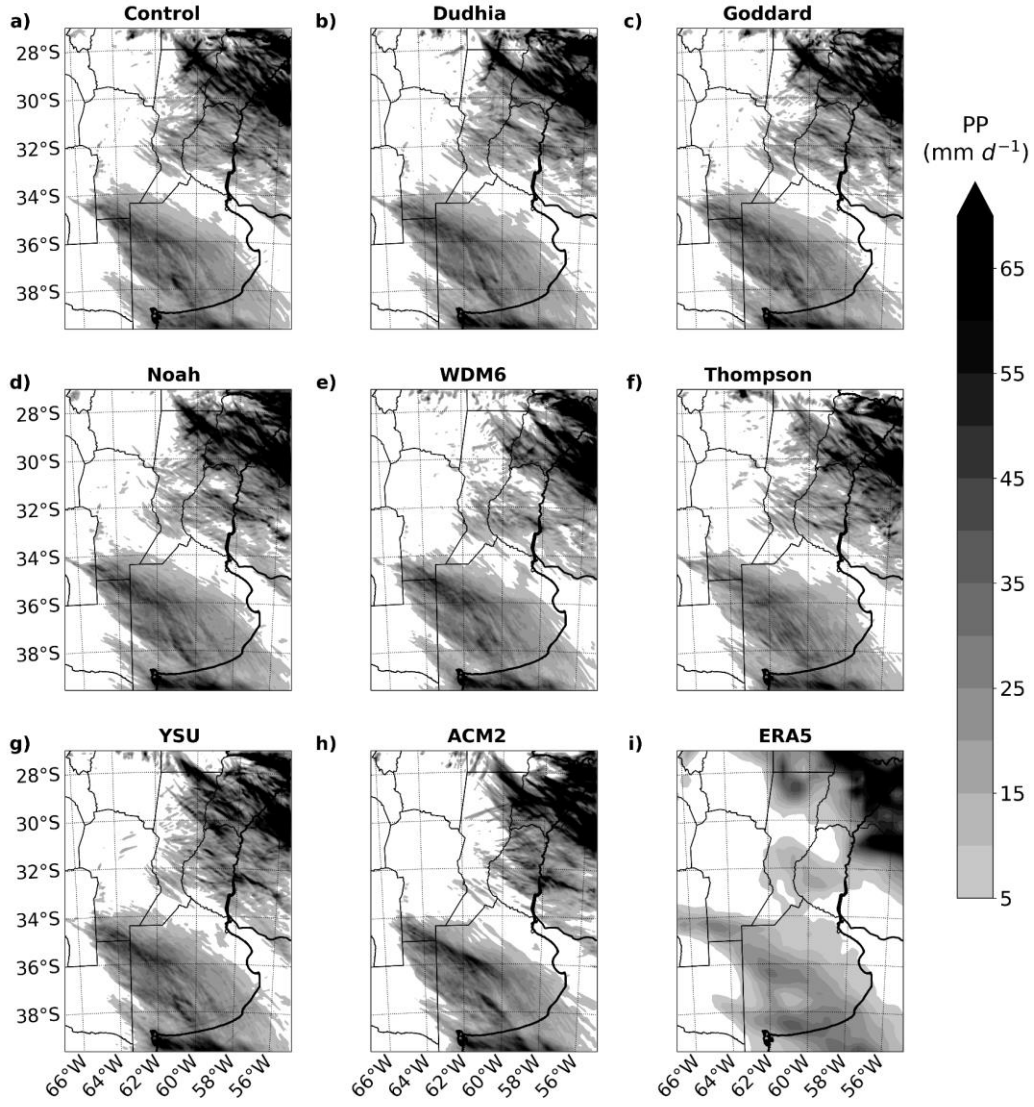

Fig. S10: 24-hour accumulated PP during the rainy case in the inner domain.

5. Soundings

Here we present the individual soundings used in the study. The sounding sites where the simulations differed the most were in Córdoba at 23:00 hours UTC in the sunny and cloudy cases and in Villa María del Río Seco and Córdoba at 18:00 hours UTC during the rainy case (Fig. S11-S13). From the same figures, it can be seen that ERA5 was worse than most of the models when simulating inversions like in Ezeiza at 12:00 hours UTC during the cloudy and rainy cases. It is important to highlight that the WRF resolution of the results was downscaled to ERA5 vertical levels to allow a fairer comparison of the results. Therefore, the WRF configurations outperformed ERA5 in simulating inversions, but ERA5 had equal or better results in the other situations.

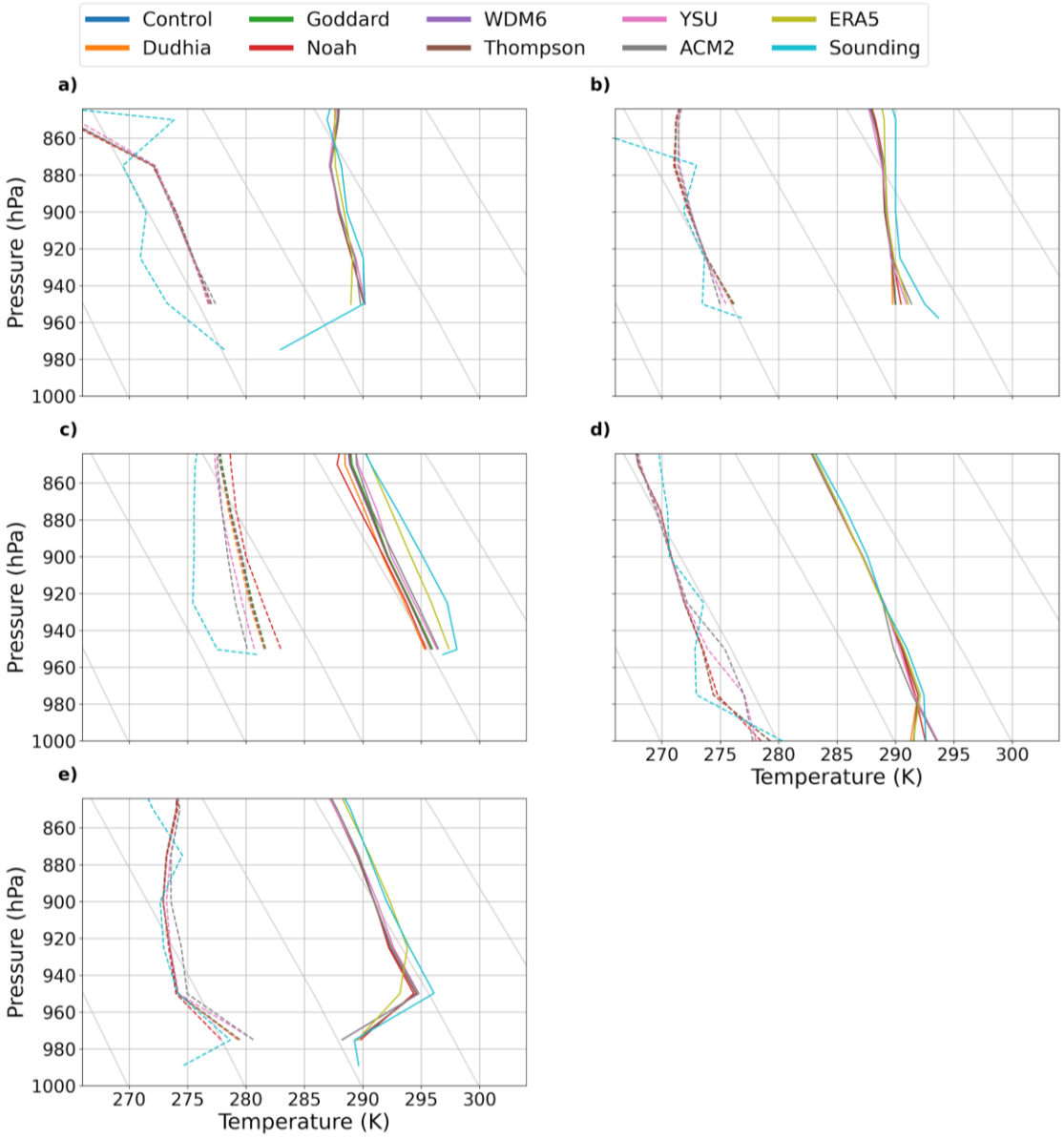

Fig. S11. Dry (solid) and dew (dotted) temperatures along the ABL from the weather soundings and model outputs during the sunny case. The locations and times were a) Villa María del Río Seco at 8:30:24 hours UTC, Córdoba at b) 11:27:55 and c) 23:28:52 hours UTC, d) Ezeiza at 11:37:31 and e) Santa Rosa at 11:11:27 hours UTC.

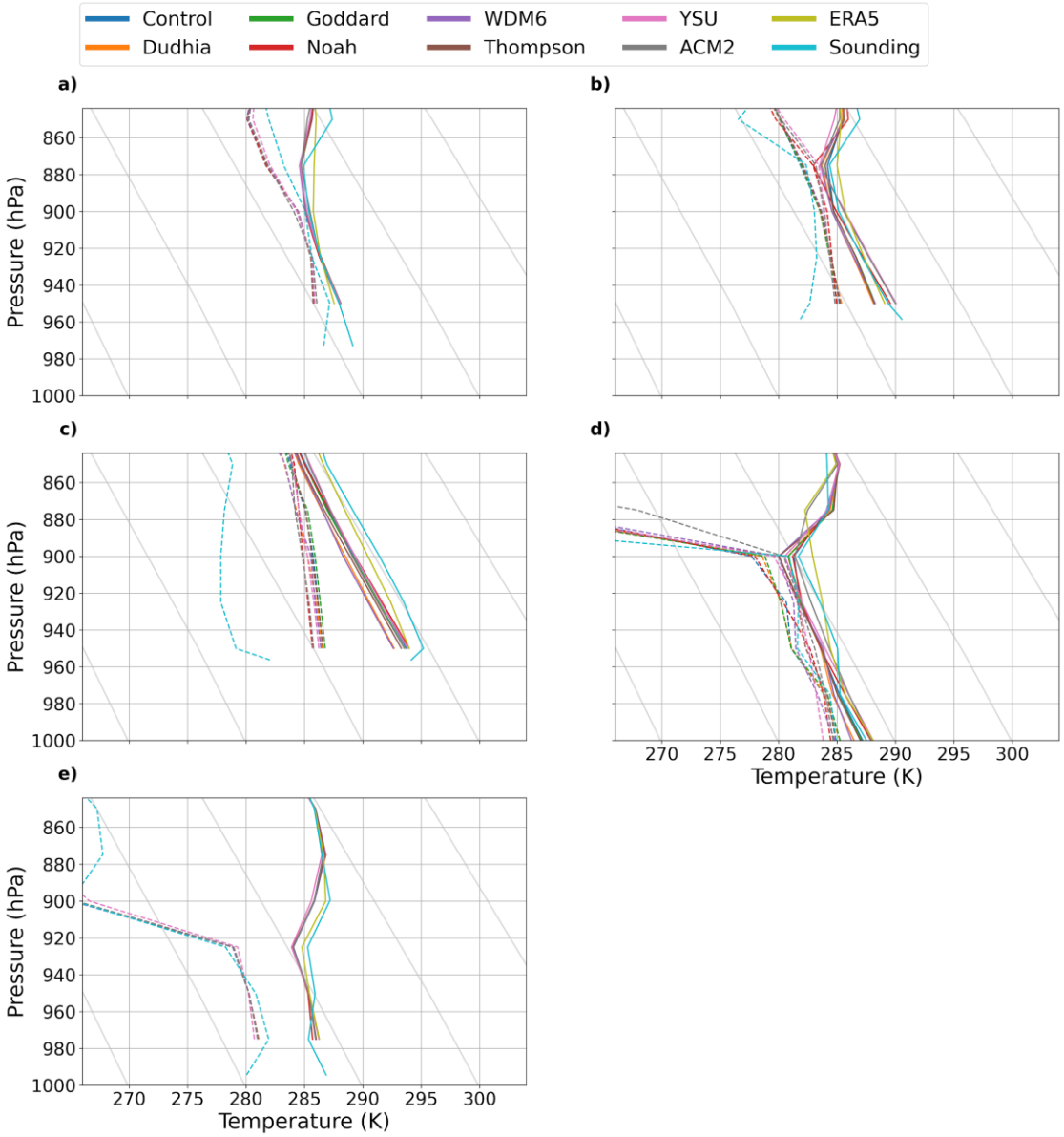

Fig. S12. Dry (solid) and dew (dotted) temperatures along the ABL from the weather soundings and model outputs during the cloudy case. The locations and times were a) Villa María del Río Seco at 8:30:24 hours UTC, Córdoba at b) 11:27:55 and c) 23:28:52 hours UTC, d) Ezeiza at 11:37:31 and e) Santa Rosa at 11:11:27 hours UTC.

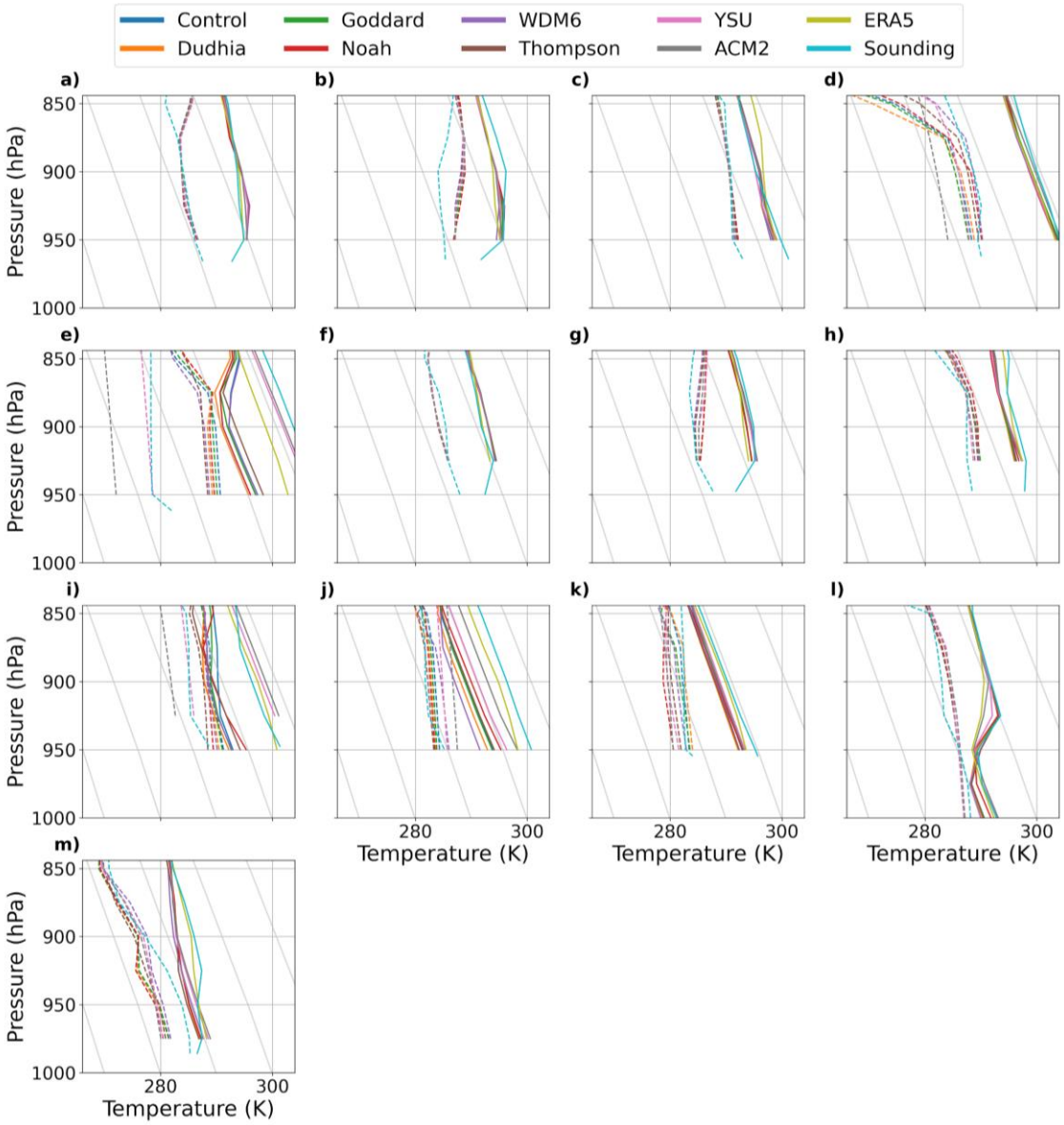

Fig. S13. Dry (solid) and dew (dotted) temperatures along the ABL from the weather soundings and model outputs during the rainy case. The locations and times were Villa María del Río Seco at a) 05:30:56, b) 8:27:02, c) 11:31:47, d) 14:31:19 and e) 17:30:02 hours UTC, Córdoba at f) 05:31:17, g) 8:30:42, h) 11:30:26, i) 14:31:23, j) 17:30:13 and k) 23:30:30 hours UTC, l) Ezeiza at 11:38:08 and m) Santa Rosa at 11:11:33 hours UTC.